buildings

Article

Research on Dynamic Pile-Driving Formula Parameters and Driving Feasibility of Extra-Long PHC Pipe Piles

Xiaomin Liu, Yonggang Xiao *, Junlong Zhou, Longbo Ge and Ziwen Song

Technical Center, China Construction Sixth Engineering Bureau Corp., Ltd., Tianjin 300012, China
* Correspondence: xiaoyonggang2010@163.com

Abstract: Prestressed high-strength concrete (PHC) pipe pile has the advantages of high single pile bearing capacity, a wide range of applications, good driving resistance, fast construction speed, etc. It has been widely used in high-rise buildings, bridges, ports, and other industries. The application of extra-long PHC pipe piles with a length of more than 50 m is increasing. However, there are few studies on the drivability and hammering criteria of extra-long PHC piles. To analyze the drivability of extra-long piles and predict their bearing capacity, in this paper, high-strain dynamic tests were carried out on 14 test sections with the pile foundation of Temburong Bridge in Brunei as the research background. The hammer stop control criteria calculated according to the Hiley formula would lead to excessive hammering. Three types of damage occurred during construction: pile shaft breakage, weld tearing, and pile head breakage. The weight and drop height of the piling hammer selected for this project were appropriate, and the extra-long test piles can be hammered to the design depth. The values of C_p (Compression of the pile) and n (the efficiency of the blow) were fitted based on the dynamic test data, which provided a more accurate reference for the selection of subsequent piling parameters of the project. It provides a more accurate calculation method for predicting the bearing capacity of extra-long PHC piles and provides control criteria for pile stopping and a scientific basis for their design and construction.

Keywords: PHC pipe piles; driving feasibility; dynamic pile-driving formula; high-strain dynamic test

Citation: Liu, X.; Xiao, Y.; Zhou, J.; Ge, L.; Song, Z. Research on Dynamic Pile-Driving Formula Parameters and Driving Feasibility of Extra-Long PHC Pipe Piles. *Buildings* **2023**, *13*, 1302. https://doi.org/10.3390/buildings13051302

Academic Editors: Suraparb Keawsawasvong, Yongqiang Zhou, Erdi Abi, Longlong Lv and Shaobo Chai

Received: 24 March 2023
Revised: 5 May 2023
Accepted: 11 May 2023
Published: 16 May 2023

1. Introduction

A pile load test can control the piling quality and verify whether the pile design is reasonable, and promote the continuous development of foundation design and construction practice [1–8]. The traditional prestressed high-strength concrete (PHC) pipe pile has the advantages of the high bearing capacity of a single pile, wide application range, good driving resistance, and fast construction speed. At present, it has been widely used in high-rise buildings, bridges, ports, and other industries [9–15].

High-strain dynamic testing has been widely used in engineering piles, has achieved good results, and has also been generally recognized by the engineering community. During the whole process of PHC pile driving, the pile-driving wave equation can be used to simulate and calculate important information such as the bearing capacity of a single pile, the tensile and compressive stress of the pile body, and the number of blows, so as to help the designer verify and determine the pile type and bearing capacity required by the project [16–20]. After the high-strain pile-driving test, the feasibility analysis can be carried out to obtain the estimated values of the tensile and compressive stress change of the pile body, pile-driving resistance, and bearing capacity [21]. The feasibility analysis can simulate the pile stress during the pile-driving process and provide a basis for the selection of pile-driving equipment. In addition to detecting the integrity of the pile body, the high-strain method can also detect the vertical compressive bearing capacity of a single pile. Zhang et al. carried out high strain detection and static load tests on the pile foundation of an offshore wind power project [22]. The results showed that the number of simulated hammer blows by the high-strain method was similar to the actual hammer blows, which proved the reliability of the high-strain piling procedure to analyze the vertical compressive load-bearing capacity of pile foundations. Liu et al. collected the high-strain method and static load method test results of 76 PHC pipe piles in the field for comparison [23]. The results showed that 84.2% of the tested piles had the bearing capacity error of the high-strain method controlled within ±10%. Some of the bearing capacity measured by the high-strain method was greater than the bearing capacity of the static load method, and some were less than the bearing capacity of the static load method. The probability of these two situations occurring was roughly the same. Therefore, the high-strain method can accurately test the piling effect of engineering piles, and it can be used to optimize the pile design and piling process in the pile test stage and engineering piling stage.

Using the relevant measured data of the high-strain method, the relevant parameters of the Hiley formula can be calculated. A typical expression of the Hiley formula is as follows:

$$P_u = WHn/(S + C/2) \tag{1}$$

Zhang et al. compared the predicted geotechnical pile-bearing capacity using the Hiley formula and the high-strain method [24], and the results showed that the pile-bearing capacity values derived from the Hiley formula were consistently lower than those derived from the high-strain method and static load tests. Triantafyllidis proposed a simple method to calculate the mass of moving piles under impact action and compared the results of this method with an example of long pile construction in Hong Kong. Four formulas including Hiley's formula were used to estimate the pile-bearing capacity by Arsyad et al. The results showed that the calculated values of Hiley's formula were underestimated. Four formulas including Hiley's formula were used to estimate the pile-bearing capacity by Arsyad et al. [25]. The results showed that the calculated values of Hiley's formula were underestimated. Tokhi proposed a method to improve the widely used Hiley kinetic equation, which can evaluate the bearing capacity of piles more accurately [26].

In summary, it can be seen that the Hiley formula does not accurately predict the bearing capacity of piles, and for extra-long piles, the predicted values are even more inaccurate. There are few studies on the drivability and hammering criteria of extra-long PHC piles. It is essential to explore the pile-driving formula applicable to using hydraulic hammers to drive extra-long piles. In order to analyze the drivability of super-long piles and predict their bearing capacity, in this paper, high-strain dynamic tests were carried out on 14 test sections with the pile foundation of Temburong Bridge in Brunei as the research background.

The Temburong Sea-crossing Bridge in Brunei crosses Brunei Bay, which connects the Brunei-Muara area and the Temburong area, as shown in Figure 1. This line is 30 km in length, of which the CC4 bid section is 12 km in length, including 940 spans of fully prefabricated viaducts, 25 spans of partially prefabricated viaducts, and 3 spans of cast-in-place continuous beam bridges. The CC4 bid section crosses the virgin forest protection area. There are many swamps, and the weak layer is thicker. Most of the bridge bases are precast tubular piles, and their pile numbers are P269 to P1209. The rocks near P1209 are relatively shallow. The outer diameter of the prefabricated pipe piles is 900 mm, and the inner diameter is 620 mm, with a total of 7536. Its total length is about 5.5×10^5 m, the average length is about 72 m, and the longest is 90 m. All piles were driven by hydraulic hammering.

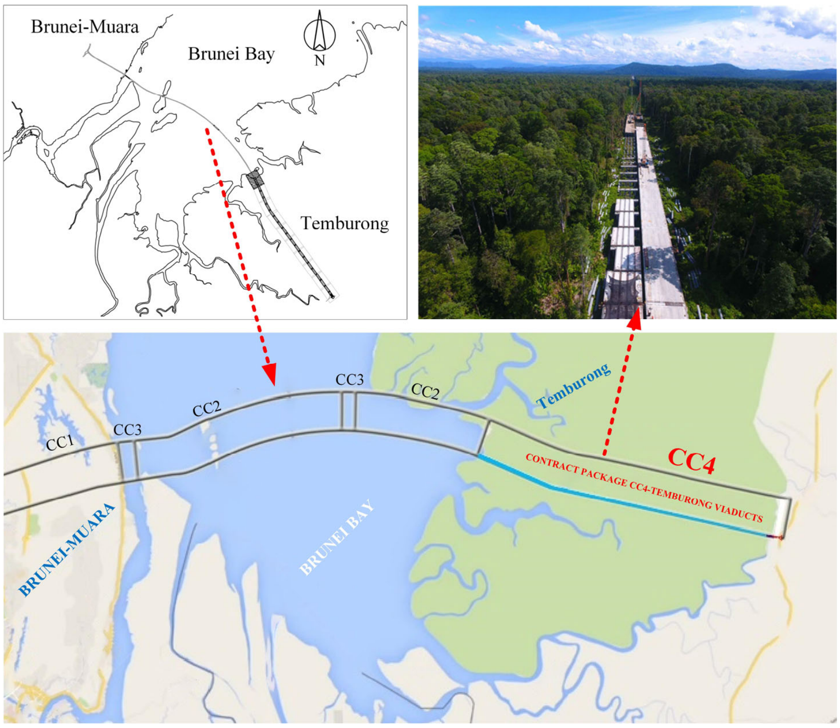

Figure 1. The geographical location of the Brunei Temburong bridge.

2. Materials and Methods

A test section of piling was carried out prior to the piling of the Brunei Temburong Bridge. High-strain dynamic load tests were carried out for extra-long PHC pipe piles to test and record the pile penetration, elastic deformation, bearing capacity, hammering efficiency, and other parameters. The pile number of the prefabricated pipes pile was P269 to P1237, and 14 test sections were set at different locations. There were 14 piers in the test section, marked as PPT1–PPT14. All piles in the test section were tested using the high-strain dynamic method during the hammering and sinking of the piles. The location and work direction of 14 test piles is shown in Figure 2. The whole line was divided into 4 working faces for construction. They were P269–P516, P754–P517, P755–P989, and P1237–P990. The P269, P754, and P1237 were three starting working faces.

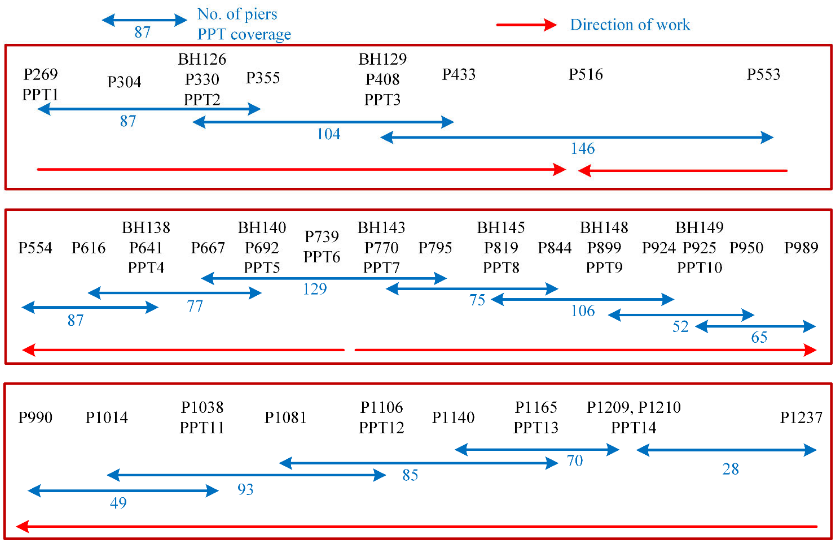

Figure 2. The location and work direction of 14 test piles.

2.1. Piling Dynamic Load Tests [27]

Dynamic load tests are used to provide on-site estimates of the bearing capacity of piles. The Pile Driving Analyzer (PDA) system is specially used for dynamic load testing and drive monitoring.

Dynamic monitoring is achieved by installing two sets of sensors at the pile head. Strain and acceleration sensors (two of each type) are installed below the pile head. These sensors are directly installed on the opposite sides of the pile above the ground. After connecting the strain and acceleration sensors to the pile head and PDA system, these sensors record the relationship between the pile top force and velocity with time when the pile head is vertically hammered. This information is stored for future redisplay and further analysis.

The PDA program records parameters including estimated driving resistance, estimated static resistance, energy transmitted through sensors, and many other parameters. The details of the test pile are shown in Table 1. From the table, it can be seen that the hammers that provide impact force for dynamic load tests are hydraulic hammers of 200 kN and 160 kN, with a drop distance of 0.6 m to 1.2 m and a pile length of 39 m to 80 m.

Table 1. The details of the test piles.

Pile Number	Pile Length (m)	AS-Build Toe Level (m)	Holding Layer	Hammer Weight (kN)	Drop Height (m)	DVL (kN)
PPT1	78	−70.0	Stiff clay	200	0.9	3000
PPT2	80	−76.0	Hard clay	200	0.9	3000
PPT3	80	−75.5	Dense sand	200	0.9	3000
PPT4	70	−65.3	Stiff clay	200	0.9	2600
PPT5	68	−60.7	Dense sand	200	0.9	2600
PPT6	78	−69.3	Dense sand	200	1.2	2600
PPT7	59	−52.3	Dense sand	200	0.9	2600
PPT8	72	−64.7	Stiff clay	200	0.9	2600
PPT9	70	−59.2	Medium dense sand	200	0.9	2600
PPT10	69	−60.2	Stiff clay	200	0.9	2600
PPT11	59	−50.4	Hard clay	160	0.9	2400
PPT12	55	−45.0	Hard clay	160	0.9	2400
PPT13	58	−44.2	Stiff clay	160	0.9	2400
PPT14	39	−34.4	Mudstone	160	0.6	2400

Where DVL is Design Verification Load.

The instruments and equipment for this high-strain test included hammering equipment, sensors, signal acquisition, and analyzers. The connection diagram of testing instruments and equipment is shown in Figure 3. The hammering equipment used was the hammer used for driving PHC pipe piles. The installation of two acceleration sensors and two strain sensors met the specification requirements.

The CAPWAP analysis program uses wave equations to analyze pile-driving parameters, which are used to calculate pile movement and stress during the pile-driving process. Using the CAPWAP program, the force and speed of hammering recorded in the selected field were used as the input of signal matching. The CAPWAP program established a pile-soil model to analyze and recorded pile-top force/time and pile-top velocity/time parameters. The model of the pile consisted of a block mass, springs, dampers, and surrounding soil. The CAPWAP program calculated parameters such as force and velocity of the model pile, and then compared them with actual measured parameters such as force and velocity. If the difference between the two was large, the pile model and the soil resistance model were continuously adjusted until a good match was obtained. Once the matching was achieved, a good dynamic model of the pile can be obtained. Then, this dynamic model will be used to determine the distribution of pile parameters along the length direction of the pile, and the CAPWAP program can be used to predict the load and settlement of the pile.

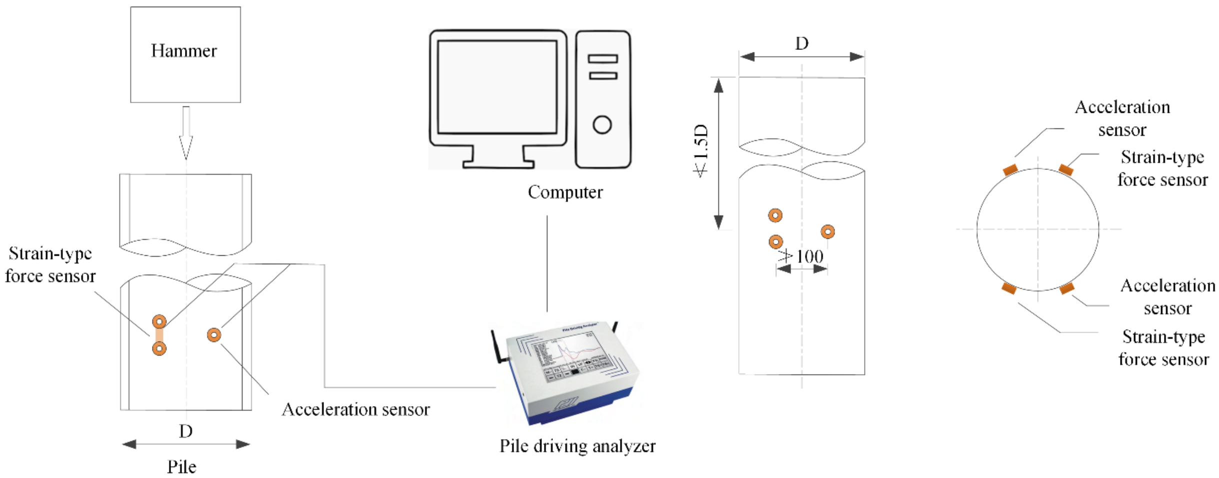

Figure 3. The connection diagram of testing instruments and equipment.

In this test, the base piles of 14 piers were performed as a high-strain dynamic test. The test parameters of the test piles are shown in Table 1.

2.2. The Calculation of the Final Set (S)

Among many pile-driving formulas provided in the literature, the Hiley formula is the most commonly used pile-driving formula at present. When it is impossible to determine the stopping standard by field pile test, the reference value of final penetration can be determined according to the calculation results of the Hiley formula and the driving experience value of similar pile foundation conditions. The Hiley formula is expressed as follows:

$$P_u = \frac{k \times W \times H}{S + (C_c + C_p + C_q)/2} \times \frac{W + e^2 \times W_p}{W + W_p} \tag{2}$$

The formula needs to measure the temporary compression (C_p) of the pile and the temporary compression value (C_q) of the soil mass at the end of the last 10 blows at the end of pile driving. The maximum bearing capacity of the pile can be calculated according to the actual pile length and the measured elastic compression value of the pile and soil (C_p + C_q). If the design bearing capacity of the pile is not greater than the calculated value, the required bearing capacity of the pile is considered to be met.

In this project, when the final set reaches the preset value, in order to conduct high-strain dynamic tests, two sensors were installed symmetrically at the top of the piles. Through the sensor, the force and acceleration of piles can be obtained under dynamic loads. According to PDA analysis of related data, it is easy to obtain factors such as pile stress, hammer energy, and ultimate bearing capacity of piles. According to the data obtained by the dynamic measurement, the parameter η value in the Hiley formula (the effective transfer coefficient of the hammer energy) and the C (the total elastic deformation of the pile-soil system) value can be calculated.

The final set (S) of this project was determined by the Hiley formula, and its expression was as follows.

$$S = \frac{kWH(W + e^2 W_p)}{P_u (W + W_p)} - \frac{C_c + C_p + C_q}{2} \tag{3}$$

In this table, k is the mechanical efficiency of the hammer, which represents the reduction coefficient of falling hammer efficiency [28–30]. When the hammer is an ideal free-fall hammer, k = 1; when the hammer is not freely falling, k < 1, usually k = 0.8~0.9. e is the coefficient of restitution, defined as the ratio of the initial velocity and the final velocity of the material after impact. e is 0.25 for reinforced-concrete piles with helmets, and e is 0.5 for steel piles. However, for PHC pipe piles, the specifications do not specify how to select e. Based on engineering experience, e is taken between 0.35 and 0.5.

Take the pipe pile with a pile length of 76 m and a bearing capacity of 4620 kN as an example to calculate the S value under different falling distances. During the S value calculation, multiple parameters need to be assumed. For this project, it is assumed that k is 0.8, e is 0.35, and H is 1.0–1.5 m. The calculation results are shown in Table 2. The E' is effective hammer energy per blow, and its value is kWH. The C is $C_c + C_p + C_q$. It can be seen from the table that the calculation value of S is 36.7 mm to 45.7 mm.

Table 2. Calculation of the final set of piles at a different drop height.

Length (m)	H (m)	E' (kN.m)	C (mm)	S (mm)	Notes
76	1.0	128.0	7	44.8	P_u = 4620 kN W = 160 kN W_p = 689 kN k = 0.8 e = 0.35
76	1.1	140.8	10	37.7	
76	1.2	153.6	10	45.7	
76	1.3	166.4	12	43.7	
76	1.4	179.2	15	36.7	
76	1.5	192.0	16	39.6	

In order to clearly clarify the relationship between the final set and the height of the falling hammer, Formula (2) is represented by different curves, as shown in Figure 4. It can be seen from the figure that for piles with the same parameters such as L, k, e, and other parameters, the final set increases with the height of the falling hammer. The calculation value of the final set decreases with the elastic deformation of the pile-soil system. However, for on-site piling, it is very inconvenient to use Table 2 or Figure 4 to determine the final set. After the parameters of P_u, k, and e are given assumptions, it is very convenient to make a form to query the final set, as shown in Table 3. This form can query the final set under different pile lengths and different elastic compression.

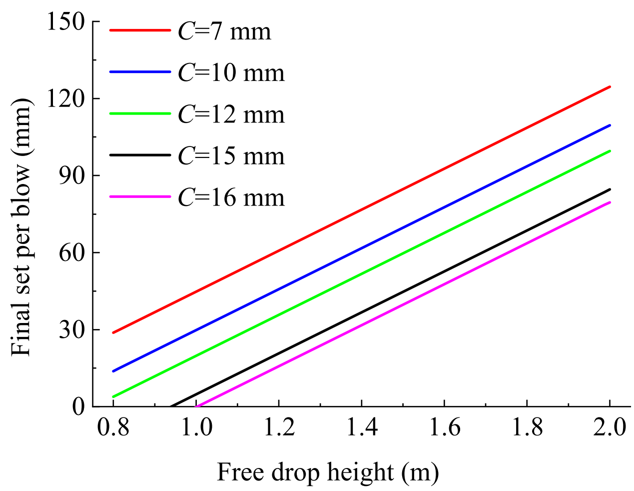

Figure 4. Relationship between final set per blow and free drop height.

Table 3 is applicable to W = 200 kN, H = 1.0 m, and P_u = 4620 kN. The set values are obtained based on assumed ($C_p + C_q$) = (9–18) mm. The assumed ($C_p + C_q$) value will be verified when the actual ($C_p + C_q$) value is obtained on-site later. The C_c value takes 3 mm and k takes 0.8. When a driving cap with cushion is used, e is 0.35. In the table, the value of n is $(W + W_p \times e^2)/(W + W_p)$. Taking L = 76 m as an example, the calculated final set is 35 mm if $C_p + C_q$ = 12 mm is assumed.

Table 3. Proposed set values table based on pile lengths and selected (C_p + C_q).

Pile Length (m)	n	Temporary Compression (C_p + C_q mm)									
		9	10	11	12	13	14	15	16	17	18
50	0.387						49	44	39	34	29
51	0.384						47	42	37	32	27
52	0.381						46	41	36	31	26
53	0.377					50	45	40	35	30	25
54	0.374					49	44	39	34	29	
55	0.371					48	43	38	33	28	
56	0.368					47	42	37	32	27	
57	0.365					46	41	36	31	26	
58	0.362				50	45	40	35	30	25	
59	0.359				49	44	39	34	29		
60	0.357				48	43	38	33	28		
61	0.354				47	42	37	32	27		
62	0.351				46	41	36	31	26		
63	0.349			50	45	40	35	30	25		
64	0.346			49	44	39	34	29			
65	0.344			49	44	39	34	29			
66	0.341			48	43	38	33	28			
67	0.339			47	42	37	32	27			
68	0.337			46	41	36	31	26			
69	0.334		50	45	40	35	30	25			
70	0.332		50	45	40	35	30	25			
71	0.330		49	44	39	34	29				
72	0.328		48	43	38	33	28				
73	0.326		47	42	37	32	27				
74	0.324		47	42	37	32	27				
75	0.322		46	41	36	31	26				
76	0.320	50	45	40	35	30	25				
77	0.318	50	45	40	35	30	25				
78	0.316	49	44	39	34	29					
79	0.314	48	43	38	33	28					
80	0.312	48	43	38	33	28					

In the Hiley formula, n is the efficiency of the blow, which represents the ratio of energy after impact to the striking energy of the ram [31,32]. The expression is as follows:

$$n = \frac{W + e^2 W_p}{W + W_p} = \frac{1 + e^2 W_p / W}{1 + W_p / W} \tag{4}$$

When $W > W_p e$ or

$$n = \frac{W + e^2 W_p}{W + W_p} - \left(\frac{W - e W_p}{W + W_p} \right)^2 \tag{5}$$

When $W < W_pe$. For extra-long PHC pipe piles, the selection of parameter n is not applicable. Therefore, it is necessary to study a simple and applicable method for obtaining n values.

3. Results and Discussion

3.1. Results and Analysis of Dynamic Load Pile-Driving Tests

When the final set meets the hammer requirements, the pile analyzer (referred to as PDA) was used for dynamic testing to test whether the bearing capacity of the pile reaches the design standard. Otherwise, it is necessary to continue driving the pile until the bearing capacity meets the design requirements.

The dynamic load test was used to provide field estimates of the mobilized static load-carrying capacity of the piles. In addition, it can be used to check pile structural integrity and to obtain field data for later computer signal matching to determine capacity and soil resistance. The S and (C_p + C_q) values were determined by conventional manual measurement methods. The pile penetration record was a curve drawn by a pencil where the workers were near the target pile. The pencil tracked the motion of the pile on a piece of paper under the driver's hammer, as shown in Figure 5. The on-site staff explained the figure to check whether the piling results were in accordance with the final penetration derived from the pile formula. Otherwise, the piling must be repeated and tested until the results are satisfactory. If the actual penetration is not greater than the calculated value of S, it is considered that the penetration of the pile meets the requirements. Taking the PPT1 pile as an example, the calculated S value according to the formula is 57 mm, while as shown in Figure 5, the actual recorded S value during pile driving is 48 mm. Obviously, the penetration of this pile meets the calculation requirements.

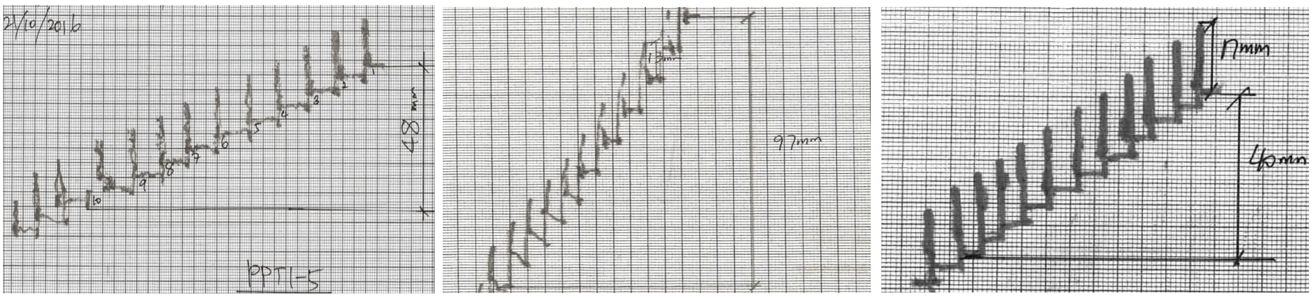

Figure 5. Piling penetration record of partial test piles.

The dynamic test results of the test piles are shown in Table 4.

Table 4. The test results of the test piles.

Pile Number	S (mm)	$C_p + C_q$ (mm)	CSX (MPa)	TSX (MPa)	EMX (kN·m)	P_u (kN)	ETR (%)
PPT1	48	15	15.6	3.8	45	4726	31.8
PPT2	177	18	28.2	4.8	96	3677	53.3
PPT3	115	12	24.0	3.0	59	3966	32.8
PPT4	57	10	31.1	1.4	120	5414	66.7
PPT5	78	12	28.0	1.1	103	7337	57.2
PPT6	81	16	41.8	2.8	184	6560	76.4
PPT7	97	13	35.3	3.6	152	5368	84.4
PPT8	40	17	36.7	5.1	150	5327	83.3
PPT9	54	14	25.7	1.7	104	4658	57.8
PPT10	39	15	30.0	3.1	114	6349	63.3
PPT11	33	11	28.8	7.4	68	4764	47.2
PPT12	42	9	35.9	4.3	137	5030	95.1
PPT13	102	10	37.8	4.0	122	5445	84.7
PPT14	35	10	14.4	1.3	86	4761	89.6

Where: EMX is Maximum Energy Transferred to the pile; CSX is Maximum Compression Stress; TSX is Maximum Tension Stress; ETR is Hammer Efficiency.

It can be seen from Table 4 that the maximum value of the final entry S value is 177 mm, and the minimum value is 33 mm. According to the design requirements, the ultimate compressive bearing capacity of the piles should be greater than 2 times the DVL. It can be seen from the table that the P_u value of most piles is greater than 2 times DVL. After 28 days of rest, the ultimate bearing capacity of all piles can meet the design requirements. It can be seen from Table 4 that the maximum value of the final set (S) value is 177 mm, and the minimum value is 33 mm. The changing range of the S value is large, and the distribution is more discrete. The variation of the $C_p + C_q$ value is from 9 to 18 mm, and its distribution is relatively concentrated. In addition, under the same driving conditions, the hammering efficiency varies greatly. In addition, there was a large difference in hammering efficiency under the same driving conditions.

3.2. Analysis of Driving Feasibility

The maximum compressive stress of the pile shaft refers to the maximum compressive stress generated by the hammering force at the top of the pile. There are many influencing factors, including pile length, pile section, pile materials, soil, pile cushion, pile hammer weight, and drop height. Reasonable control of the maximum stress in the pile can prevent the pile from being cracked. The maximum value of CSX is 41.8 MPa, and the maximum value of TSX is 7.4 MPa. The concrete grade used for the PHC pipe piles in this project was C50. None of the maximum compressive stresses exceeded the ultimate compressive strength of concrete, while the maximum tensile stresses in some of the piles exceeded the ultimate tensile strength of concrete. Under repeated hammering action, some of the pile heads or pile bodies were damaged. A total of three types of damage were found to have occurred during construction by means of PDA tests and visual observation: pile shaft breakage, weld tearing, and pile head breakage, as shown in Figure 6. The occurrence of these failures during the pile testing process was caused by various reasons, including hammer deflection, insufficient penetration, and unsuitable pile pads. The pile hammer was hydraulically driven, with the oil pipe hanging on one side, causing the hammer body to tilt due to unilateral pulling. The axis of the hammer deviates significantly from the axis of the PHC pipe pile, causing severe shaking of the pile body during construction. In addition, some parameters in the Hiley formula have assumed values that differ significantly from the actual values, resulting in the calculated penetration S value being too small. Furthermore, some pile cushion materials used paper cushions, which contained 17 layers of paper. Through practical testing, the effectiveness of the paper cushion is not good, and it is easy to burn under high impact temperatures, which can cause uneven thickness of the pile cushion, resulting in an uneven hammering force on the pile head.

(**a**) (**b**) (**c**)

Figure 6. Failure types of the PHC pipe pile driving. (**a**) Pile shaft breakage; (**b**) Weld tearing; (**c**) Pile head breakage.

Before piling, every 0.25 m on the pile body was marked, and the number of blows per 0.25 m would be automatically recorded by the instrument. The number of blows in each group of test piles had a good correlation, and the number of blows in the same group of test piles was very close. The relationship between the stratigraphic parameters; the number of pile-driving hammer blows; and the depth for PPT1, PPT6, and PPT14 piles is shown in Figure 7. In general, the hammer blow per unit pile length increased with the increase in depth. However, it can be seen from Figure 7 that the number of hammer blows per unit pile length does not simply increase with depth. The geological conditions of each pile were different, and the corresponding Standard Penetration Test (SPT) value curve was also different. As can be seen from the figure, when the geological conditions are hard clay, dense sand, and weathered rock, the SPT value increases significantly, and the corresponding number of pile-driving hammer blows also increases significantly. The hammer weight of the PPT1 pile was 200 kN, the drop height was 0.7 m, the pile bottom elevation was −70 m, the hammer stop penetration S was 4.8 mm/blow, the total number of blows was 4728, the maximum compressive stress was 15.6 MPa, the maximum tensile stress was 3.8 MPa, and the compressive bearing capacity was 4726 kN. With this hammer type, the test pile PPT1 can be basically driven in place. The hammer weight of the PPT6 pile was 200 kN, the height of hammer fall was 1.2 m, the elevation of the pile bottom was −69.3 m, the stopping hammer penetration S was 8.1 mm/hammer blow, the total number of hammer blows was 5134, the maximum compressive stress was 41.8 MPa, the maximum tensile stress was 2.8 MPa, and the compressive bearing capacity was 6560 kN. The hammer weight of the PPT14 pile was 160 kN, the height of hammer fall was 0.6 m, the elevation of the pile bottom was −34.4 m, the stopping hammer penetration S was 3.5 mm/hammer blow, the total number of hammer blows was 1889, the maximum compressive stress was 14.4 MPa, the maximum tensile stress was 1.3 MPa, and the compressive bearing capacity was 4761 kN. It can be seen from the figure that the number of blows per meter corresponding to different depths is closely related to the properties of corresponding soil layers. In hard clay, dense sand, and weathered rock strata, the number of blows per unit pile length increases significantly.

3.3. Parameter Analysis of the Hiley Formula

Several parameters in Hiley's formula (such as hammer efficiency k, coefficient of restitution e, compression of pile cushion C_c, pile-soil elastic deformation ($C_p + C_q$)) were determined by assumptions, hence the final hammer penetration S obtained by Hiley's formula may differ significantly from the actual situation. The comparison between the measured and calculated values of the ultimate compressive bearing capacity of the single pile is shown in Table 5. The S_m in the table is the measured value, while S_p is the proposed set of values for stopping hammering. The S_p was calculated using Hiley's formula based on the design values of the bearing capacity and the assumed parameters. Most of the piles at the construction site did not meet the penetration requirements calculated according to the Hiley formula for stopping the hammer. As can be seen from Table 5, S_m is greater than S_p, especially since the difference between the two values of the PPT6 pile is large. The P_{um} in the table is the ultimate value of compressive bearing capacity measured by dynamic load tests, while P_{ud} is the design value. As can be seen from the table, although the final stopping hammering set S_m does not reach the requirement of S_p calculated according to Hiley's formula, the P_{um} values are all greater than the P_{ud} values and meet the design bearing capacity requirements. In order to meet the requirements of S_p calculated by the Hiley formula, excessive hammering would occur during pile driving on site, resulting in damage to the pile head, pile tip, and pile body.

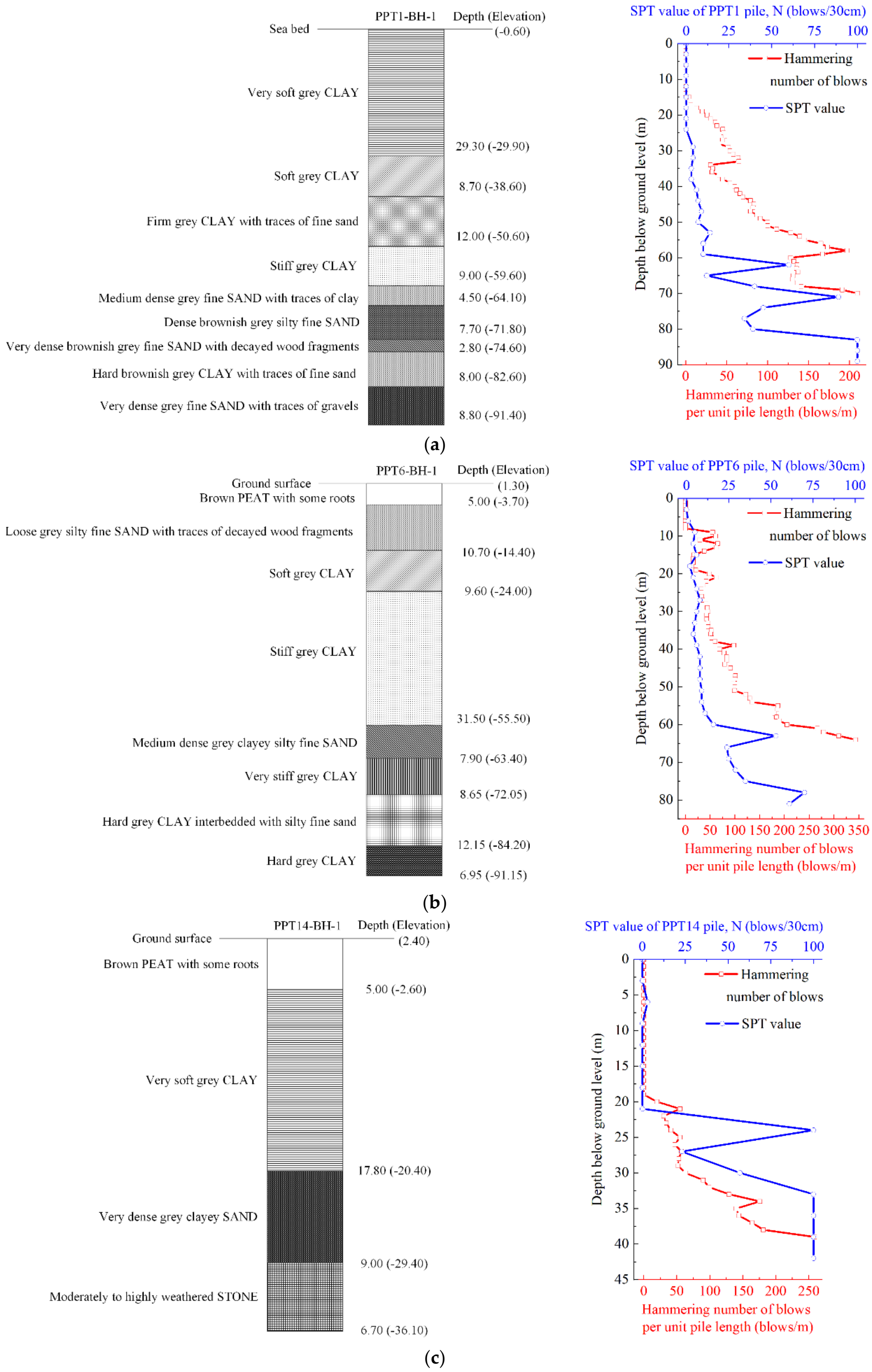

Figure 7. Strata parameter and monitoring of pile-driving blow count; (**a**) PPT1; (**b**) PPT6; (**c**) PPT14.

Table 5. Comparison between measured and calculated values of ultimate compressive bearing capacity of a single pile.

Pile No.	L (m)	H (m)	S_m (mm)	S_p (mm)	$C_p + C_q$ (mm)	C_c (mm)	P_{um} (kN)	P_{ud} (kN)	Percent Difference (%)
PPT6-1	78	1.2	81	21	14	3	6720	5200	29.23
PPT6-3	65	1.1	86	18	23	3	5980	5200	15.00
PPT6-5	65	1.1	114	18	16	3	6580	5200	26.54
PPT14-1	37	1.0	99	86	15	3	5190	4400	17.95
PPT14-2	39	0.6	24	21	13	3	4950	4400	12.50
PPT14-3	39	0.6	35	21	10	3	5230	4400	18.86

In order to analyze the differences in the values taken for the parameters of the Hiley formula, a comparison of the calculated and actual values of C_c, C_{p+q}, and e is presented in Table 6. According to the Hiley formula, C_c was taken as 3 mm in the calculation of this project. The C_c-C in the table is the positive arithmetic value, while C_c-B is the inverse arithmetic value introduced from the piling results. The Pd-C_c is the percentage difference between C_c-C and C_c-B. As can be seen from the table, the difference between the two values is relatively large, especially for the PPT14 pile, the C_c-B is surprisingly negative. The C_{p+q}-C in the table is the positive arithmetic value, while C_{p+q}-M is the dynamic load test measured value. The Pd-C_{p+q} is the percentage difference between C_{p+q}-C and C_{p+q}-M. The minimum value of Pd-C_{p+q} is 9.69% and the maximum value is 48.57%. According to the Hiley formula, e was taken as 0.5 in the calculation of this project. The e-C in the table is the positive arithmetic value, while e-B is the inverse arithmetic value introduced from the piling results. The Pd-e is the percentage difference between e-C and e-B. The minimum value of Pd-e is 25.60% and the maximum value is 72.20%. According to the Hiley formula parameter-taking method published by the British Institution of Civil Engineers, the values of C_c and C_q were determined by the pile material and the difficulty of pile driving. The value of C_p was taken not only related to these two factors but also related to the pile length. The values of C_c and C_q were small, and the ratio of C_c and C_q to all temporary compression was very low. The easier it was to sink the pile, the smaller the values of these two values were. The value of C_p was taken to be proportional to the pile length and accounted for a high ratio of all temporary compressions. Most of the PHC pipe piles in this project were extra-long piles, of which more than 93% were over 50 m in length. The pile length has a great influence on the C_p value, however, there are very few studies on the C_p value of extra-long PHC pipe piles.

Table 6. Comparison of calculated and actual values for C_c, C_{p+q}, and e.

Pile No.	C_c-C (mm)	C_c-B (mm)	Pd-C_c (%)	C_{p+q}-C (mm)	C_{p+q}-M (mm)	Pd-C_{p+q} (%)	e-C	e-B	Pd-e (%)
PPT6-1	3	5.23	74.33	20.80	14	48.57	0.5	0.759	51.80
PPT6-3	3	6.41	113.67	17.55	23	23.70	0.5	0.857	71.40
PPT6-5	3	0.84	72.00	17.55	16	9.69	0.5	0.796	59.20
PPT14-1	3	−3.15	205.00	10.55	15	29.67	0.5	0.628	25.60
PPT14-2	3	−10.67	455.67	11.05	13	15.00	0.5	0.668	33.60
PPT14-3	3	−7.15	338.33	11.05	10	10.50	0.5	0.861	72.20

The pile lengths and C_p values of all test piles in this project were counted and the relationship between the two was linearly fitted, as shown in Figure 8. The correlation coefficient R^2 is 0.7953, and the correlation between the two is good. As can be seen from Figure 8, for extra-long PHC pipe piles over 50 m, the relationship between C_p and pile length L is:

$$C_p = 0.36L - 11.37 \tag{6}$$

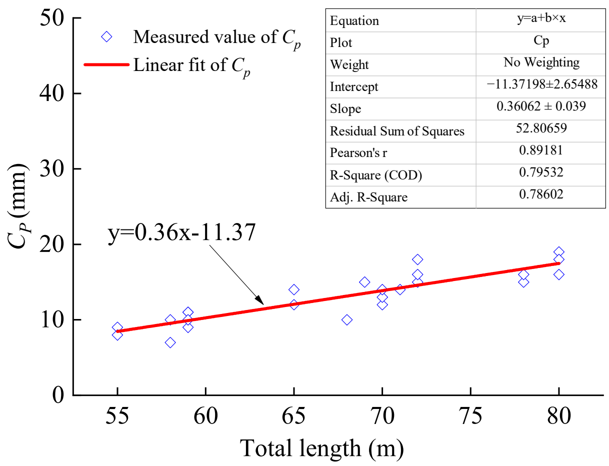

Figure 8. Fitting relationship between C_p and pile length.

The value of n is related to e and W_p/W, where e is the coefficient of restitution, and W_p/W is the ratio of pile weight to hammer weight. In this project, the minimum value of W_p/W of piles with a length of more than 50 m was 2.71, and the maximum value was 3.62. Within such a small range of variation, W_p/W had little influence on the value of n, corresponding to a minimum value of 0.41 and a maximum value of 0.45 for n. Therefore, a small range of W_p/W values has little effect on n values.

For piles with a longer length, the value of coefficient n in the Hiley formula is smaller. It means that the energy transferred from the hammer to the pile is very small. The reason is that the quality of the whole pile is considered. If the pile is relatively long, only the part of the pile body affected by the hammer should be considered during the process of bearing the hammer. However, it is very difficult to determine the length of the part of the pile body affected by the hammer. The coefficient of restitution and hammering efficiency have a very close correlation. The hammering efficiency data of the test piles in this project were counted and the relationship between them was fitted, as shown in Figure 9. The correlation coefficient R^2 is 0.9843, and the correlation between the two is good. As can be seen from Figure 9, for extra-long PHC pipe piles over 50 m, the relationship between n and e is:

$$n = 111.94e - 15.43 \tag{7}$$

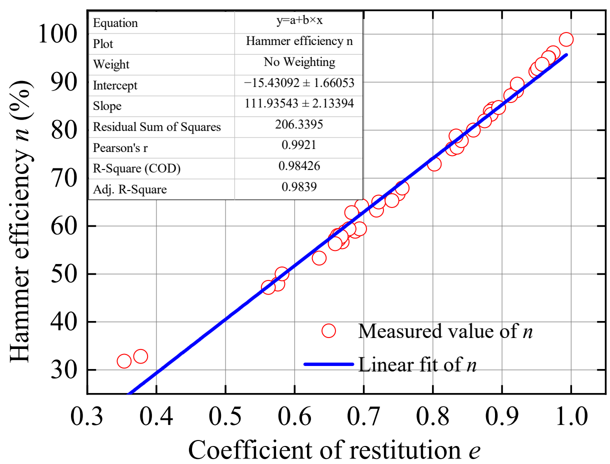

Figure 9. Fitting the relationship between hammer efficiency and the coefficient of restitution.

The value of the coefficient of restitution, e, was determined by the pile material and the piling conditions. According to the Hiley formula parameter value method published by the British Society of Civil Engineers, the value of e is 0.4 when the PHC pipe pile was driven by the single-acting hammer pile driver, and the value of e is 0.5 with a double-acting hammer. However, the coefficient of restitution of most piles in this project was greater than 0.5. The number of e greater than 0.5 accounts for 95.65% of all test piles. Obviously, this is quite different from the initial assumed value of e. With the development of piling technology, in addition to the steam hammer and diesel hammer, the hydraulic piling hammer has been widely used. The piling equipment used in this project was the hydraulic hammer. The hydraulic hammer does not emit any waste gas, has no noise, and has a high impact frequency. Each impact can achieve greater penetration. However, the value of e is not clear when the hydraulic hammer is used for the extra-long pile. Generally, in order to determine the penetration and verify whether the piling equipment, construction technology, and technical measures are suitable, the piling technology test must be carried out before the pile-driving construction. Therefore, the selection of the e value of super-long piles should be determined according to the test data of different pile lengths, different geological conditions, and different pile sinking techniques.

4. Conclusions

In this study, the extra-long PHC pipe pile was taken as the research object, and its driving resistance and pile-driving parameters were tested on the construction site. The following conclusions can be drawn.

- The hammer stop control criteria calculated according to the Hiley formula would lead to excessive hammering, with some piles having maximum tensile stresses exceeding the ultimate tensile strength of the concrete. Three types of damage occurred during construction: pile shaft breakage, weld tearing, and pile head breakage;
- The weight and drop height of the piling hammer selected for this project were appropriate, and the extra-long test piles can be hammered to the design depth. The number of blows per meter corresponding to different depths was closely related to the properties of corresponding soil layers. In hard clay, dense sand, and weathered rock strata, the number of blows per unit pile length increased significantly;
- In order to avoid pile damage caused by excessive hammering, the driving parameters of extra-long piles should be adjusted according to the high-strain dynamic test data. In this paper, the values of C_p and n were fitted based on the dynamic test data, which provided a more accurate reference for the selection of subsequent piling parameters of the project.

Author Contributions: Conceptualization, Y.X. and X.L.; methodology, Y.X. and X.L.; writing—review and editing, Y.X., X.L., J.Z., L.G. and Z.S.; project administration and funding acquisition, X.L. All authors have read and agreed to the published version of the manuscript.

Funding: This research was funded by the Science and Technology Research and Development Project of China State Construction Engineering Group Co., Ltd., grant number CSCEC-2020-Z-21.

Data Availability Statement: The data used to support the findings of this study are included in the article.

Conflicts of Interest: The authors declare no conflict of interest.

Nomenclature

P_u	ultimate bearing capacity of pile
k	mechanical efficiency of hammer
W, W_p	weight of hammer and pile
H	free drop height
e	coefficient of restitution
e-C	e value used for calculating S_p
e-B	backcalculation value of e based on test
S	penetration of pile per hammer blow

S_m	measured value of penetration
S_p	proposed value of penetration
C	summation of the temporary compression
C_c	compression of pile cushion
C_c-C	assumed value of C_c used for calculating S_p
C_c-B	backcalculation value of C_c based on test
C_p	compression of pile
C_q	compression of quake
C_{p+q}	sum of C_p and C_q
C_{p+q}-C	C_{p+q} value used for calculating S_p
C_{p+q}-M	measured value of C_{p+q} based on test
n	efficiency of the blow

References

1. Abadie, C.N.; Byrne, B.W.; Houlsby, G.T. Rigid pile response to cyclic lateral loading: Laboratory tests. *Geotechnique* **2019**, *69*, 863–876.
2. Flynn, K.N.; McCabe, B.A. Driven cast-in-situ pile capacity: Insights from dynamic and static load testing. *Can. Geotech. J.* **2021**, *58*, 1870–1883. [CrossRef]
3. Han, F.; Ganju, E.; Salgado, R.; Prezzi, M. Comparison of the load response of closed-ended and open-ended pipe piles driven in gravelly sand. *Acta Geotech.* **2019**, *14*, 1785–1803. [CrossRef]
4. Kou, H.L.; Chu, J.; Guo, W.; Zhang, M.Y. Pile load test of jacked open-ended prestressed high-strength concrete pipe pile in clay. *Proc. Inst. Civ. Eng. -Geotech. Eng.* **2018**, *171*, 243–251. [CrossRef]
5. Lanyi-Bennett, S.A.; Deng, L.J. Axial load testing of helical pile groups in glaciolacustrine clay. *Can. Geotech. J.* **2019**, *56*, 187–197. [CrossRef]
6. McAdam, R.A.; Byrne, B.W.; Houlsby, G.T.; Beuckelaers, W.; Burd, H.J.; Gavin, K.G.; Igoe, D.J.P.; Jardine, R.J.; Martin, C.M.; Wood, A.M.; et al. Monotonic laterally loaded pile testing in a dense marine sand at Dunkirk. *Geotechnique* **2020**, *70*, 986–998. [CrossRef]
7. Santrac, P.; Susic, N.; Bajic, Z. Determination of the Pile Stiffness Matrix Based on the Pile Load Test Results and the Effect of Pile Interaction. *Teh. Vjesn.-Tech. Gaz.* **2020**, *27*, 2016–2023.
8. Wang, S.; Lei, X.W.; Meng, Q.S.; Xu, J.L.; Wang, M.Z.; Guo, W. Model tests of single pile vertical cyclic loading in calcareous sand. *Mar. Georesources Geotechnol.* **2021**, *39*, 670–681. [CrossRef]
9. Cao, X.L.; Dai, G.L.; Gong, W.M.; Zhu, M.X.; Tang, J.A. Experimental study on the seismic behavior of new PHC piles. *Arab. J. Geosci.* **2020**, *13*. [CrossRef]
10. Huynh, V.H.; Nguyen, T.; Nguyen, D.P.; Nguyen, T.S.; Huynh, T.M.D.; Nguyen, T.C. A novel direct SPT method to accurately estimate ultimate axial bearing capacity of bored PHC nodular piles with 81 case studies in Vietnam. *Soils Found.* **2022**, *62*, 101163. [CrossRef]
11. Kou, H.L.; Chu, J.; Guo, W.; Zhang, M.Y. Field study of residual forces developed in pre-stressed high-strength concrete (PHC) pipe piles. *Can. Geotech. J.* **2016**, *53*, 696–707. [CrossRef]
12. Kou, H.L.; Guo, W.; Zhang, M.Y. Field study of set-up effect in open-ended PHC pipe piles. *Mar. Georesources Geotechnol.* **2017**, *35*, 208–215. [CrossRef]
13. Li, X.S.; Zhang, J.Q.; Xu, H.; Shi, Z.W.; Gao, Q.F. Static Load Test and Numerical Analysis of Influencing Factors of the Ultimate Bearing Capacity of PHC Pipe Piles in Multilayer Soil. *Sustainability* **2021**, *13*, 13166. [CrossRef]
14. Nguyen, T.; Ly, K.D.; Nguyen-Thoi, T.; Nguyen, B.P.; Doan, N.P. Prediction of axial load bearing capacity of PHC nodular pile using Bayesian regularization artificial neural network. *Soils Found.* **2022**, *62*, 101203. [CrossRef]
15. Oktiovan, Y.P.; Otaki, T.; Obara, T.; Kono, S.; Asai, Y.; Kobayashi, K.; Watanabe, H.; Mukai, D. Shear performance evaluation of PHC piles under different levels of axial load ratio. *Earthq. Eng. Struct. Dyn.* **2022**, *51*, 2091–2112. [CrossRef]
16. Meng, Q.J.; Shi, Z.F. Vibration Isolation of Plane Waves by Periodic Pipe Pile Barriers in Saturated Soil. *J. Aerosp. Eng.* **2019**, *32*, 11. [CrossRef]
17. Salgado, R.; Zhang, Y.B.; Abou-Jaoude, G.; Loukidis, D.; Bisht, V. Pile driving formulas based on pile wave equation analyses. *Comput. Geotech.* **2017**, *81*, 307–321. [CrossRef]
18. Wu, W.B.; El Naggar, M.H.; Abdlrahem, M.; Mei, G.X.; Wang, K.H. New interaction model for vertical dynamic response of pipe piles considering soil plug effect. *Can. Geotech. J.* **2017**, *54*, 987–1001. [CrossRef]
19. Zheng, C.J.; Ding, X.M.; Sun, Y.F. Vertical Vibration of a Pipe Pile in Viscoelastic Soil Considering the Three-Dimensional Wave Effect of Soil. *Int. J. Geomech.* **2016**, *16*, 10. [CrossRef]
20. Zheng, C.J.; Liu, H.L.; Ding, X.M.; Zhou, H. Vertical vibration of a large diameter pipe pile considering transverse inertia effect of pile. *J. Cent. South Univ.* **2016**, *23*, 891–897. [CrossRef]
21. Sun, Y.; Gao, Y.; Zhang, J.; Hu, J.; Huang, W. Feasibility analysis and field test on driving phc pile through deep dense sand. *J. Eng. Geol.* **2015**, *23*, 1079–1084.

22. Zhang, H.; He, R.; Chen, Q.; Xiao, J.; Chu, Y. Comparative evaluation of theoretical method and in situ tests method on vertical compressive bearing capacity of super-large-diameter monopiles for offshore wind turbines. *Ocean Eng.* **2022**, *40*, 104–115.
23. Liu, C.; Tang, M.; Hu, H.; Chen, H.; Liu, C.; Hou, Z. Comparative study on vertical compressive bearing behavior of PHC pipe piles based on high strain method and static load method. *Build. Struct.* **2022**, *52*, 136–140.
24. Zhang, L.; Chau, A.C.W.; Shek, M.P. Bearing capacity of long driven piles using dynamic methods. In Proceedings of the 12th Asian Regional Conference on Soil Mechanics and Geotechnical Engineering (12ARC), Singapore, 4–8 August 2003.
25. Arsyad, A.; Suyadi; Samang, L. Statistical Analysis of Dynamic Bearing Capacity of Driven Pile. In Proceedings of the 2nd International Conference on Civil, Offshore and Environmental Engineering (ICCOEE), Kuala Lumpur, Malaysia, 3–5 June 2014.
26. Tokhi, H.; Ren, G.; Xie, Y.M. Improving the Predictability of Hiley Pile Driving Formula in the Quality Control of the Pile Foundation. In Proceedings of the International Conference on Civil Engineering and Building Materials (CEBM), Kunming, China; 2011.
27. Xiao, Y.; Liu, X.; Zhou, J.; Song, L. Field Test Study on the Bearing Capacity of Extra-Long PHC Pipe Piles under Dynamic and Static Loads. *Sustainability* **2023**, *15*, 5161. [CrossRef]
28. Chellis, R.D. *Pile Foundations*; McGraw Hill: New York, NY, USA, 1961.
29. Chan, W.T.; Chow, Y.K.; Liu, L.F. Neural network: An alternative to pile driving formulas. *Comput. Geotech.* **1995**, *17*, 135–156. [CrossRef]
30. Goh, A.T.C. Back-propagation neural networks for modeling complex systems. *Artif. Intell. Eng.* **1995**, *9*, 143–151. [CrossRef]
31. El-Mossallamy, Y.M.; Tawfik, M.M.; Zayed, M.A. Application of ultimate limit state design for axially loaded single piles in Egyptian geotechnical practice. *HBRC J.* **2015**, *13*, 181–189. [CrossRef]
32. Sun, L.; Jia, T.; Yan, S.; Guo, W.; Ren, Y.; Lei, Z. Prediction of pile running during the driving process of large diameter pipe piles. *Ocean Eng.* **2016**, *128*, 48–57. [CrossRef]